JOURNAL OF MOLECULAR SPECTROSCOPY 172, 407–420 (1995)

Far-Infrared Spectrum of HO_2

K. V. CHANCE,* K. PARK,† K. M. EVENSON,‡ L. R. ZINK,§ AND F. STROH¶

*Harvard–Smithsonian Center for Astrophysics, Cambridge, Massachusetts 02138; †Department of Physics, University of Oregon, Eugene, Oregon 97403; ‡National Institute for Standards and Technology, Boulder, Colorado 80303; §Cooperative Institute for Research in Environmental Sciences, NOAA and University of Colorado, Boulder, Colorado 80303; and ¶Institute for Stratospheric Chemistry, Forschungszentrum Jülich, 0-52425, Jülich, Germany

We have measured the frequencies of 17 transitions in the far-infrared spectrum of the hydroperoxyl radical, HO_2, from 2.5 to 5.9 THz, encompassing rotational levels up to $N = 19$ and $K_{-1} = 5$. These measured transition frequencies are combined with previously measured microwave and millimeter-wave transition frequencies in a complete reanalysis of the HO_2 Hamiltonian for the ground vibrational state, including spin–rotation and nuclear hyperfine interactions. A revised set of molecular constants is presented. These include centrifugal distortion effects through octic dependence on the rotational angular momentum and the off-diagonal tensor component of the spin–spin dipolar interaction between the proton and the unpaired electron spin.

1. INTRODUCTION

The hydroperoxyl radical, HO_2, is important spectroscopically as a prototypical light, asymmetric radical. In recent years its environmental importance has become obvious as well: HO_2 and OH are the radical pair that are the catalysts in one of the three major cycles of destruction of stratospheric ozone. Additionally, HO_2 is an important constituent in the oxidation chemistry of the earth's troposphere, which regulates tropospheric ozone production and loss. The measurements presented here were undertaken primarily to provide a firm spectroscopic basis for the radiative transfer calculations involved in the analysis of far-infrared and millimeter-wave atmospheric measurements of HO_2, including the measurement of HO_2 itself and the analysis for interference from HO_2 in the measurements of other species.

Stratospheric HO_2 has proved difficult to measure due to its low abundance and the lack of suitably strong infrared absorption features. Spectroscopic measurements are now made by remote sensing using far-infrared and submillimeter-wave emission spectroscopy from balloons (*1–3*), and by *in situ* chemical conversion of HO_2 to OH, followed by laser-induced fluorescence (*4*). Satellite-based submillimeter-wave measurements of stratospheric HO_2 are also planned as part of the NASA Earth Observing System (Eos) (*5*). Ground-based remote-sensing measurements have been made utilizing millimeter-wave emissions (*6*).

The lowest-lying microwave transitions of HO_2, near 65 GHz, were first measured in the laboratory by Beers and Howard (*7*). These transitions were remeasured at higher accuracy by Saito (*8*), who extended the measurements to 136 GHz. Millimeter-wave measurements by Charo and De Lucia (*9*) further extended the set of measurements to 520 GHz. The previous line listing generally used for remote sensing measurements of HO_2 is the JPL Submillimeter, Millimeter, and Microwave Spectral Line Catalog, revision 3 (JPL) (*10*), which is based on the measurements of Saito and of

0022-2852/95 $12.00

Charo and De Lucia. The present work extends the frequency measurements for HO_2 lines up to 5.9 THz (196 cm^{-1}). These measurements are combined with the previous microwave and millimeter-wave measurements into a data set that is fitted simultaneously to a parameterized Hamiltonian expression described below. The combined data set contains the transitions used in ground-based millimeter-wave measurements and five of the nine transitions currently used in the far-infrared balloon measurements. The transitions used in balloon-borne submillimeter-wave sensing and proposed for Eos are not measured directly in this work; the transition frequencies are, however, determined more accurately from the fitting to the Hamiltonian expression in the present study.

HO_2 is also of considerable interest in astrophysics. The present work permits more accurate determination of the frequencies of transitions that are candidates for astronomical measurements, particularly the lowest *b*-type transitions, near 626 GHz.

2. EXPERIMENTAL SUMMARY

HO_2 is produced in a fast flow system as in Ref. (*11*), by reacting chlorine atoms with methanol to produce CH_2OH, followed by reaction with O_2 to produce HO_2:

$$Cl + CH_3OH \rightarrow CH_2OH + HCl$$

$$CH_2OH + O_2 \rightarrow HO_2 + H_2CO$$

$$\text{Net: } Cl + CH_3OH + O_2 \rightarrow HO_2 + HCl + H_2CO. \qquad (1)$$

The optimum conditions for production of HO_2 are as given in Ref. (*11*); the present study, in fact, began at an earlier time and produced the conditions for formation of maximum $[HO_2]$ that were later used in pressure-broadening studies.

The line frequencies were measured using the TuFIR technique of laser-mixing spectroscopy, in which tunable far-infrared radiation of extremely high spectral purity and accuracy (ca. 10 kHz (*12*)) is generated by the nonlinear mixing of radiation from 2 CO_2 lasers and a microwave source (*13, 14*).

3. DATA ANALYSIS AND RESULTS

Line positions are determined by nonlinear least-squares fitting of the measured spectra to modulation-broadened Voigt derivative lineshapes, as described previously (*15, 16*). The uncertainties given for the transition frequencies include the uncertainty from the spectrum fitting process, plus an additional 10 kHz (1σ) added in quadrature to account for uncertainty in the far-infrared frequencies synthesized by the TuFIR technique (*16*).

In order to perform an analysis with maximum predictive capability, we decided to perform a simultaneous fitting to the Hamiltonian expression using all of the zero-field frequency measurements of HO_2 that we are aware of. The microwave frequencies included in the present fitting are from the study of Saito (*8*). The uncertainties given in that study are adopted directly. The millimeter-wave frequencies are from the study of Charo and De Lucia (*9*). We have taken the 1σ uncertainties for the transition frequencies to be 0.1 MHz (De Lucia, private communication, 1990), which is consistent with the rms fitting result of 0.084 MHz obtained in their study. Table I gives the measured frequencies, the 1σ uncertainties, and, as discussed below, the fitted frequencies for the combined list of 175 transitions included in this study. Several typographical errors in the published frequencies and assignments for the millimeter-

TABLE I

Rotational Transitions of HO_2 (MHz)[a]

N′	K'_{-1}	K'_1	J′	F′	N″	K''_{-1}	K''_1	J″	F″	Observed[b]	Calculated[b]	O-C	(O-C)[c]	N′	K'_{-1}	K'_1	J′	F′	N″	K''_{-1}	K''_1	J″	F″	Observed[b]	Calculated[b]	O-C	(O-C)[c]
7	1	7	15/2	8	8	0	8	17/2	9	27 474.24(06)	27 474.27	-0.03	0.46	3	2	2	5/2	3	2	2	1	3/2	2	184 194.55(10)	184 194.57	-0.02	0.17
7	1	7	15/2	7	8	0	8	17/2	8	27 477.69(04)	27 477.60	0.09	2.16	3	2	2	5/2	2	2	2	1	3/2	1	184 196.76(10)	184 196.80	-0.04	0.39
7	1	7	13/2	6	8	0	8	15/2	7	35 530.88(03)	35 530.83	0.05	1.65	3	2	1	5/2	3	2	2	0	3/2	2	184 212.64(10)	184 212.65	-0.01	0.09
7	1	7	13/2	7	8	0	8	15/2	8	35 535.41(04)	35 535.38	0.03	0.72	3	2	1	5/2	2	2	2	0	3/2	1	184 214.87(10)	184 214.91	-0.04	0.38
9	0	9	17/2	9	8	1	8	15/2	8	37 138.59(07)	37 138.45	0.14	2.04[d]	11	0	11	21/2	11	10	1	10	19/2	10	184 373.81(10)	184 373.98	-0.17	1.72
9	0	9	17/2	8	8	1	8	15/2	7	37 142.60(05)	37 142.54	0.06	1.26	11	0	11	21/2	10	10	1	10	19/2	9	184 378.30(10)	184 378.32	-0.02	0.23
9	0	9	19/2	9	8	1	8	17/2	8	44 069.56(04)	44 069.60	-0.04	1.09	25	1	24	51/2	25	24	2	23	49/2	24	186 590.82(10)	186 590.86	-0.04	0.40
9	0	9	19/2	10	8	1	8	17/2	9	44 073.10(10)	44 072.92	0.18	1.80[d]	25	1	24	51/2	26	24	2	23	49/2	25	186 594.26(10)	186 594.20	0.06	0.60
1	0	1	3/2	1	0	0	0	1/2	0	65 070.85(08)	65 070.88	-0.03	0.33	3	1	3	5/2	3	2	1	2	3/2	2	188 350.71(10)	188 350.80	-0.09	0.92
1	0	1	3/2	2	0	0	0	1/2	1	65 081.82(04)	65 081.81	0.01	0.19	3	1	3	5/2	2	2	1	2	3/2	1	188 351.58(10)	188 351.60	-0.02	0.19
1	0	1	3/2	1	0	0	0	1/2	1	65 098.44(09)	65 098.41	0.03	0.39	11	0	11	23/2	11	10	1	10	21/2	10	189 596.64(10)	189 596.71	-0.07	0.73
1	0	1	1/2	1	0	0	0	1/2	0	65 373.01(10)	65 373.05	-0.04	0.44	11	0	11	23/2	12	10	1	10	21/2	11	189 600.00(10)	189 599.98	0.02	0.23
1	0	1	1/2	0	0	0	0	1/2	1	65 396.15(10)	65 396.31	-0.16	1.61	3	1	2	5/2	2	2	1	1	3/2	2	193 937.06(10)	193 937.20	-0.14	1.40
1	0	1	1/2	1	0	0	0	1/2	1	65 400.63(10)	65 400.58	0.05	0.47	3	1	2	5/2	2	2	1	1	3/2	1	193 939.56(10)	193 939.66	-0.10	1.01
6	1	6	13/2	7	7	0	7	15/2	8	98 117.82(05)	98 117.78	0.04	0.87	3	1	2	5/2	3	2	1	1	3/2	2	193 940.83(10)	193 940.87	-0.04	0.37
6	1	6	13/2	6	7	0	7	15/2	7	98 121.15(05)	98 121.13	0.02	0.39	3	1	3	7/2	3	2	1	2	5/2	2	195 219.25(10)	195 219.21	0.04	0.35
6	1	6	11/2	5	7	0	7	13/2	6	107 635.51(10)	107 635.54	-0.03	0.29	3	1	3	7/2	4	2	1	2	5/2	3	195 220.22(10)	195 220.10	0.12	1.24
6	1	6	11/2	6	7	0	7	13/2	7	107 640.22(10)	107 640.33	-0.11	1.08	3	0	3	7/2	3	2	0	2	5/2	2	195 422.64(10)	195 422.68	-0.04	0.45
10	0	10	19/2	10	9	1	9	17/2	9	110 472.20(04)	110 472.19	0.01	0.32	3	0	3	7/2	4	2	0	2	5/2	3	195 423.56(10)	195 423.50	0.06	0.56
10	0	10	19/2	9	9	1	9	17/2	8	110 476.90(07)	110 476.79	0.11	1.55	3	0	3	5/2	2	2	0	2	3/2	1	195 628.34(10)	195 628.39	-0.05	0.50
10	0	10	21/2	10	9	1	9	19/2	9	116 448.40(10)	116 448.39	0.01	0.11	3	0	3	5/2	3	2	0	2	3/2	2	195 629.55(10)	195 629.57	-0.02	0.16
10	0	10	21/2	11	9	1	9	19/2	10	116 451.73(10)	116 451.68	0.05	0.48	3	1	2	7/2	3	2	1	1	5/2	2	200 615.72(10)	200 615.73	-0.01	0.14
2	1	2	3/2	1	1	1	1	1/2	1	119 137.04(07)	119 136.97	0.07	1.05	3	1	2	7/2	4	2	1	1	5/2	3	200 617.47(10)	200 617.48	-0.01	0.08
2	1	2	3/2	2	1	1	1	1/2	1	119 153.74(04)	119 153.76	-0.02	0.42	3	2	2	7/2	3	2	2	1	5/2	2	202 869.98(10)	202 869.93	0.05	0.49
2	1	2	3/2	1	1	1	1	1/2	0	119 159.19(07)	119 159.39	-0.20	2.90	3	2	2	7/2	4	2	2	1	5/2	3	202 872.19(10)	202 872.21	-0.02	0.22
2	1	1	3/2	1	1	1	0	1/2	1	122 856.61(09)	122 856.51	0.10	1.08	3	2	1	7/2	3	2	2	0	5/2	2	202 885.94(10)	202 885.86	0.08	0.81
2	1	1	3/2	1	1	1	0	1/2	0	122 858.26(07)	122 858.00	0.26	3.78	3	2	1	7/2	4	2	2	0	5/2	3	202 888.18(10)	202 888.15	0.03	0.31
2	1	1	3/2	2	1	1	0	1/2	1	122 858.92(05)	122 858.97	-0.05	1.08	19	2	18	39/2	20	20	1	19	41/2	21	235 399.96(10)	235 400.08	-0.12	1.16
2	0	2	5/2	2	1	0	1	3/2	1	130 258.13(20)	130 257.74	0.39	1.95	19	2	18	39/2	19	20	1	19	41/2	20	235 403.51(10)	235 403.54	-0.03	0.30
2	0	2	5/2	3	1	0	1	3/2	2	130 260.07(20)	130 259.65	0.42	2.09	4	1	4	9/2	5	5	0	5	11/2	6	236 280.92(10)	236 281.08	-0.16	1.58
2	0	2	3/2	1	1	0	1	1/2	0	130 463.68(20)	130 463.85	-0.17	0.83	4	1	4	9/2	4	5	0	5	11/2	5	236 284.42(10)	236 284.51	-0.09	0.92
2	0	2	3/2	2	1	0	1	1/2	1	130 467.41(20)	130 467.69	-0.28	1.40	19	2	18	37/2	18	20	1	19	39/2	19	243 470.60(10)	243 470.58	0.02	0.23
2	1	2	5/2	2	1	1	1	3/2	1	132 959.56(08)	132 959.46	0.10	1.21	19	2	18	37/2	19	20	1	19	39/2	20	243 474.69(10)	243 474.68	0.01	0.12
2	1	2	5/2	3	1	1	1	3/2	2	132 961.99(08)	132 961.98	0.01	0.08	4	3	2	7/2	4	3	3	1	5/2	3	248 431.39(10)	248 431.21	0.18	1.84
2	1	1	5/2	2	1	1	0	3/2	1	136 492.09(12)	136 491.96	0.13	1.07	4	3	1	7/2	4	3	3	0	5/2	3				
2	1	1	5/2	3	1	1	0	3/2	2	136 495.97(09)	136 495.88	0.09	0.95	4	3	2	7/2	3	3	3	1	5/2	2	248 433.15(10)	248 433.13	0.02	0.24
5	1	5	11/2	6	6	0	6	13/2	7	167 765.03(10)	167 765.02	0.01	0.10	4	3	1	7/2	3	3	3	0	5/2	2				
5	1	5	11/2	5	6	0	6	13/2	6	167 768.28(10)	167 768.40	-0.12	1.20	4	1	4	7/2	3	5	0	5	9/2	4	250 496.86(10)	250 496.87	-0.01	0.13
5	1	5	9/2	4	6	0	6	11/2	5	179 233.33(10)	179 233.46	-0.13	1.26	4	1	4	7/2	4	5	0	5	9/2	5	250 502.47(10)	250 502.32	0.15	1.51
5	1	5	9/2	5	6	0	6	11/2	6	179 238.50(10)	179 238.52	-0.02	0.19														

TABLE I—*Continued*

N′	K'_{-1}	K'_1	J′	F′	N″	K''_{-1}	K''_1	J″	F″	Observed[b]	Calculated[b]	O-C	(O-C)[c]
4	2	3	7/2	4	3	2	2	5/2	3	253 189.10(10)	253 188.96	0.14	1.38
4	2	3	7/2	3	3	2	2	5/2	2				
4	2	2	7/2	4	3	2	1	5/2	3	253 233.72(10)	253 233.57	0.15	1.48
4	2	2	7/2	3	3	2	1	5/2	2				
4	1	4	7/2	4	3	1	3	5/2	3	254 551.53(10)	254 551.32	0.21	2.08
4	1	4	7/2	3	3	1	3	5/2	2				
4	1	4	9/2	5	3	1	3	7/2	4	258 522.94(10)	258 523.11	-0.17	1.66
4	1	4	9/2	4	3	1	3	7/2	3				
12	0	12	23/2	12	11	1	11	21/2	11	258 872.75(10)	258 872.78	-0.03	0.30
12	0	12	23/2	11	11	1	11	21/2	10	258 877.05(10)	258 876.97	0.08	0.75
4	0	4	9/2	5	3	0	3	7/2	4	260 565.86(10)	260 566.03	-0.17	1.72
4	0	4	9/2	4	3	0	3	7/2	3				
4	0	4	7/2	4	3	0	3	5/2	3	260 770.14(10)	260 769.95	0.19	1.90
4	0	4	7/2	3	3	0	3	5/2	2				
4	1	3	7/2	4	3	1	2	5/2	3	262 004.09(10)	262 003.89	0.20	1.99
4	1	3	7/2	3	3	1	2	5/2	2				
12	0	12	25/2	12	11	1	11	23/2	11	263 457.21(10)	263 457.26	-0.05	0.54
12	0	12	25/2	13	11	1	11	23/2	12	263 460.52(10)	263 460.49	0.03	0.26
4	2	3	9/2	5	3	2	2	7/2	4	265 690.53(10)	265 690.63	-0.10	1.04
4	2	3	9/2	4	3	2	2	7/2	3				
4	2	2	9/2	5	3	2	1	7/2	4	265 731.52(10)	265 731.66	-0.14	1.43
4	2	2	9/2	4	3	2	1	7/2	3				
4	1	3	9/2	4	3	1	2	7/2	3	265 769.20(10)	265 769.18	0.02	0.19
4	1	3	9/2	5	3	1	2	7/2	4	265 770.21(10)	265 770.16	0.05	0.48
26	1	25	51/2	26	25	2	24	49/2	25	268 124.79(10)	268 124.79	0.00	0.02
26	1	25	51/2	25	25	2	24	49/2	24	268 128.81(10)	268 128.81	0.00	0.04
4	3	2	9/2	4	3	3	1	7/2	3	269 498.83(10)	269 498.80	0.03	0.29
4	3	1	9/2	4	3	3	0	7/2	3				
4	3	2	9/2	5	3	3	1	7/2	4	269 500.65(10)	269 500.64	0.01	0.11
4	3	1	9/2	5	3	3	0	7/2	4				
26	1	25	53/2	26	25	2	24	51/2	25	273 013.19(10)	273 013.26	-0.07	0.66
26	1	25	53/2	27	25	2	24	51/2	26	273 016.56(10)	273 016.56	0.00	0.02
3	1	3	7/2	4	4	0	4	9/2	5	303 438.00(10)	303 438.21	-0.21	2.11
3	1	3	7/2	3	4	0	4	9/2	4	303 441.59(10)	303 441.79	-0.20	1.97
5	4	2	9/2	5	4	4	1	7/2	4	312 884.54(10)	312 884.42	0.12	1.24
5	4	1	9/2	5	4	4	0	7/2	4				
5	4	2	9/2	4	4	4	1	7/2	3	312 886.24(10)	312 886.06	0.18	1.77
5	4	1	9/2	4	4	4	0	7/2	3				

N′	K'_{-1}	K'_1	J′	F′	N″	K''_{-1}	K''_1	J″	F″	Observed[b]	Calculated[b]	O-C	(O-C)[c]
5	3	3	9/2	5	4	3	2	7/2	4	316 548.27(10)	316 548.23	0.04	0.44
5	3	2	9/2	5	4	3	1	7/2	4				
5	3	3	9/2	4	4	3	2	7/2	3				
5	3	2	9/2	4	4	3	1	7/2	3				
18	2	17	37/2	19	19	1	18	39/2	20	317 603.71(10)	317 603.76	-0.05	0.46
18	2	17	37/2	18	19	1	18	39/2	19	317 607.23(10)	317 607.24	-0.01	0.08
5	1	5	9/2	5	4	1	4	7/2	4	319 694.62(10)	319 694.48	0.14	1.43
5	1	5	9/2	4	4	1	4	7/2	3				
5	2	4	9/2	5	4	2	3	7/2	4	320 631.39(10)	320 631.34	0.05	0.51
5	2	4	9/2	4	4	2	3	7/2	3				
5	2	3	9/2	5	4	2	2	7/2	4	320 720.20(10)	320 720.14	0.06	0.59
5	2	3	9/2	4	4	2	2	7/2	3				
3	1	3	5/2	2	4	0	4	7/2	3	321 826.88(10)	321 827.11	-0.23	2.33
3	1	3	5/2	3	4	0	4	7/2	4	321 833.31(10)	321 833.20	0.11	1.12
5	1	5	11/2	6	4	1	4	9/2	5	322 242.67(10)	322 242.71	-0.04	0.43
5	1	5	11/2	5	4	1	4	9/2	4				
5	0	5	11/2	6	4	0	4	9/2	5	325 680.17(10)	325 680.18	-0.01	0.13
5	0	5	11/2	5	4	0	4	9/2	4				
5	0	5	9/2	5	4	0	4	7/2	4	325 882.22(10)	325 882.15	0.07	0.68
5	0	5	9/2	4	4	0	4	7/2	3				
18	2	17	35/2	17	19	1	18	37/2	18	326 354.31(10)	326 354.30	0.01	0.09
18	2	17	35/2	18	19	1	18	37/2	19	326 358.47(10)	326 358.45	0.02	0.20
5	1	4	9/2	5	4	1	3	7/2	4	328 995.55(10)	328 995.54	0.01	0.07
5	1	4	9/2	4	4	1	3	7/2	3				
5	2	4	11/2	6	4	2	3	9/2	5	329 373.04(10)	329 373.04	0.00	0.01
5	2	4	11/2	5	4	2	3	9/2	4				
5	2	3	11/2	6	4	2	2	9/2	5	329 456.21(10)	329 456.44	-0.23	2.27
5	2	3	11/2	5	4	2	2	9/2	4				
5	1	4	11/2	6	4	1	3	9/2	5	331 333.01(10)	331 333.06	-0.05	0.51
5	1	4	11/2	5	4	1	3	9/2	4				
5	3	3	11/2	5	4	3	2	9/2	4	332 466.93(10)	332 466.84	0.09	0.91
5	3	2	11/2	5	4	3	1	9/2	4				
5	3	3	11/2	6	4	3	2	9/2	5				
5	3	2	11/2	6	4	3	1	9/2	5				
13	0	13	25/2	13	12	1	12	23/2	12	333 936.32(10)	333 936.25	0.07	0.69
13	0	13	25/2	12	12	1	12	23/2	11	333 940.27(10)	333 940.32	-0.05	0.54
5	4	2	11/2	5	4	4	1	9/2	4	335 321.98(10)	335 322.11	-0.13	1.27
5	4	1	11/2	5	4	4	0	9/2	4				
5	4	2	11/2	6	4	4	1	9/2	5	335 323.63(10)	335 323.66	-0.03	0.30
5	4	1	11/2	6	4	4	0	9/2	5				

TABLE I—*Continued*

N'	K'_{-1}	K'_1	J'	F'	N''	K''_{-1}	K''_1	J''	F''	Observed[b]	Calculated[b]	O-C	(O-C)[c]	N'	K'_{-1}	K'_1	J'	F'	N''	K''_{-1}	K''_1	J''	F''	Observed[b]	Calculated[b]	O-C	(O-C)[c]
13	0	13	27/2	13	12	1	12	25/2	12	337 974.55(10)	337 974.57	-0.02	0.19	7	4	4	13/2	7	6	4	3	11/2	6	447 289.85(10)	447 289.87	-0.02	0.17
13	0	13	27/2	14	12	1	12	25/2	13	337 977.84(10)	337 977.76	0.08	0.82	7	4	3	13/2	7	6	4	2	11/2	6				
6	4	3	11/2	6	5	4	2	9/2	5	380 375.03(10)	380 375.04	-0.01	0.11	7	4	4	13/2	6	6	4	3	11/2	5				
6	4	2	11/2	6	5	4	1	9/2	5					7	4	3	13/2	6	6	4	2	11/2	5				
6	4	3	11/2	5	5	4	2	9/2	4					7	1	7	13/2	7	6	1	6	11/2	6	448 867.53(10)	448 867.47	0.06	0.62
6	4	2	11/2	5	5	4	1	9/2	4					7	1	7	13/2	6	6	1	6	11/2	5				
6	1	6	11/2	6	5	1	5	9/2	5	384 392.68(10)	384 392.77	-0.09	0.90	7	1	7	15/2	8	6	1	6	13/2	7	450 136.82(10)	450 137.05	-0.23	2.27
6	1	6	11/2	5	5	1	5	9/2	4					7	1	7	15/2	7	6	1	6	13/2	6				
6	1	6	13/2	7	5	1	5	11/2	6	386 147.31(10)	386 147.32	-0.01	0.15	7	3	5	13/2	7	6	3	4	11/2	6	450 374.53(10)	450 374.57	-0.04	0.41
6	1	6	13/2	6	5	1	5	11/2	5					7	3	5	13/2	6	6	3	4	11/2	5				
6	2	5	11/2	6	5	2	4	9/2	5	387 178.99(10)	387 178.98	0.01	0.13	7	3	4	13/2	7	6	3	3	11/2	6				
6	2	5	11/2	5	5	2	4	9/2	4					7	3	4	13/2	6	6	3	3	11/2	5				
6	2	4	11/2	6	5	2	3	9/2	5	387 333.95(10)	387 333.99	-0.04	0.42	7	2	6	13/2	7	6	2	5	11/2	6	453 200.48(10)	453 200.48	0.00	0.03
6	2	4	11/2	5	5	2	3	9/2	4					7	2	6	13/2	6	6	2	5	11/2	5				
6	0	6	13/2	7	5	0	5	11/2	6	390 758.87(10)	390 758.72	0.15	1.49	7	2	5	13/2	7	6	2	4	11/2	6	453 447.97(10)	453 448.03	-0.06	0.58
6	0	6	13/2	6	5	0	5	11/2	5					7	2	5	13/2	6	6	2	4	11/2	5				
6	0	6	11/2	6	5	0	5	9/2	5	390 958.21(10)	390 958.23	-0.02	0.23	7	0	7	15/2	8	6	0	6	13/2	7	455 794.60(10)	455 794.53	0.07	0.70
6	0	6	11/2	5	5	0	5	9/2	4					7	0	7	15/2	7	6	0	6	13/2	6				
6	2	5	13/2	7	5	2	4	11/2	6	393 543.30(10)	393 543.26	0.04	0.35	7	0	7	13/2	7	6	0	6	11/2	6	455 990.66(10)	455 990.63	0.03	0.25
6	2	5	13/2	6	5	2	4	11/2	5					7	0	7	13/2	6	6	0	6	11/2	5				
6	2	4	13/2	7	5	2	3	11/2	6	393 690.63(10)	393 690.62	0.01	0.10	7	2	6	15/2	8	6	2	5	13/2	7	457 994.45(10)	457 994.38	0.07	0.71
6	2	4	13/2	6	5	2	3	11/2	5					7	2	6	15/2	7	6	2	5	13/2	6				
6	1	5	11/2	6	5	1	4	9/2	5	395 535.68(10)	395 535.61	0.07	0.73	7	2	5	15/2	8	6	2	4	13/2	7	458 231.55(10)	458 231.58	-0.03	0.32
6	1	5	11/2	5	5	1	4	9/2	4					7	2	5	15/2	7	6	2	4	13/2	6				
6	3	4	13/2	6	5	3	3	11/2	5	396 034.05(10)	396 033.93	0.12	1.23	7	3	5	15/2	7	6	3	4	13/2	6	460 006.04(10)	460 005.90	0.14	1.38
6	3	3	13/2	6	5	3	2	11/2	5					7	3	5	15/2	8	6	3	4	13/2	7				
6	3	4	13/2	7	5	3	3	11/2	6					7	3	4	15/2	7	6	3	3	13/2	6				
6	3	3	13/2	7	5	3	2	11/2	6					7	3	4	15/2	8	6	3	3	13/2	7				
6	1	5	13/2	7	5	1	4	11/2	6	397 077.70(10)	397 077.75	-0.05	0.49	7	1	6	13/2	7	6	1	5	11/2	6	461 847.69(10)	461 847.92	-0.23	2.30
6	1	5	13/2	6	5	1	4	11/2	5					7	1	6	13/2	6	6	1	5	11/2	5				
6	4	3	13/2	6	5	4	2	11/2	5	398 470.75(10)	398 470.70	0.05	0.52	7	4	4	15/2	7	6	4	3	13/2	6	462 034.53(10)	462 034.58	-0.05	0.47
6	4	2	13/2	6	5	4	1	11/2	5					7	4	3	15/2	7	6	4	2	13/2	6				
6	4	3	13/2	7	5	4	2	11/2	6					7	4	4	15/2	8	6	4	3	13/2	7				
6	4	2	13/2	7	5	4	1	11/2	6					7	4	3	15/2	8	6	4	2	13/2	7				
17	2	16	35/2	18	18	1	17	37/2	19	399 022.02(10)	399 022.07	-0.05	0.49	8	0	8	17/2	9	7	0	7	15/2	8	520 780.45(10)	520 780.53	-0.08	0.79
17	2	16	35/2	17	18	1	17	37/2	18	399 025.60(10)	399 025.57	0.03	0.32	8	0	8	17/2	8	7	0	7	15/2	7				
17	2	16	33/2	16	18	1	17	35/2	17	408 517.95(10)	408 517.99	-0.04	0.40	8	0	8	15/2	8	7	0	7	13/2	7	520 972.33(10)	520 972.36	-0.03	0.28
17	2	16	33/2	17	18	1	17	35/2	18	408 522.19(10)	408 522.19	0.00	0.05	8	0	8	15/2	7	7	0	7	13/2	6				
														13	2	12	27/2	14	12	1	11	25/2	13	2 497 808.95(04)	2 497 808.98	-0.03	0.76
														13	2	12	27/2	13	12	1	11	25/2	12				

TABLE I—*Continued*

N′	K′₋₁	K′₁	J′	F′	N″	K″₋₁	K″₁	J″	F″	Observed[b]	Calculated[b]	O-C	(O-C)′[c]
14	2	13	29/2	15	13	1	12	27/2	14	2 551 119.79(05)	2 551 119.75	0.04	0.83
14	2	13	29/2	14	13	1	12	27/2	13				
9	3	6	19/2	10	9	2	7	19/2	10	2 862 042.59(18)	2 862 042.68	-0.09	0.52
9	3	6	19/2	9	9	2	7	19/2	9				
3	3	1	5/2	2	2	2	0	3/2	1	3 100 255.48(03)	3 100 255.46	0.02	0.70
3	3	1	5/2	3	2	2	0	3/2	2				
3	3	0	5/2	2	2	2	1	3/2	1				
3	3	0	5/2	3	2	2	1	3/2	2				
8	3	6	15/2	7	7	2	5	13/2	6	3 416 970.94(04)	3 416 970.97	-0.04	0.95
8	3	6	15/2	8	7	2	5	13/2	7				
16	3	14	33/2	17	15	2	13	31/2	16	3 900 150.30(07)	3 900 150.21	0.09	1.27
16	3	14	33/2	16	15	2	13	31/2	15				
16	4	12	31/2	15	16	3	13	31/2	15	4 029 030.07(10)	4 029 030.05	0.02	0.20
16	4	12	31/2	16	16	3	13	31/2	16				
19	3	17	39/2	20	18	2	16	37/2	19	4 086 471.18(05)	4 086 471.20	-0.02	0.39
19	3	17	39/2	19	18	2	16	37/2	18				
4	4	1	9/2	4	3	3	0	7/2	3	4 258 492.25(10)	4 258 492.41	-0.16	1.59
4	4	0	9/2	4	3	3	1	7/2	3				
4	4	1	9/2	5	3	3	0	7/2	4				
4	4	0	9/2	5	3	3	1	7/2	4				
4	4	1	7/2	3	3	3	0	5/2	2	4 306 810.24(08)	4 306 810.22	0.02	0.23
4	4	0	7/2	3	3	3	1	5/2	2				
4	4	1	7/2	4	3	3	0	5/2	3				
4	4	0	7/2	4	3	3	1	5/2	3				
5	4	2	11/2	6	4	3	1	9/2	5	4 324 315.59(30)	4 324 315.56	0.04	0.12
5	4	1	11/2	6	4	3	2	9/2	5				
5	4	2	11/2	5	4	3	1	9/2	4				
5	4	1	11/2	5	4	3	2	9/2	4				
5	4	2	9/2	4	4	3	1	7/2	3	4 371 260.35(1.43)	4 371 263.30	-2.95	2.06
5	4	1	9/2	4	4	3	2	7/2	3				
5	4	2	9/2	5	4	3	1	7/2	4				
5	4	1	9/2	5	4	3	2	7/2	4				
6	4	3	13/2	7	5	3	2	11/2	6	4 390 319.67(10)	4 390 319.50	0.16	1.65
6	4	2	13/2	7	5	3	3	11/2	6				
6	4	3	13/2	6	5	3	2	11/2	5				
6	4	2	13/2	6	5	3	3	11/2	5				
12	4	9	23/2	11	11	3	8	21/2	10	4 815 319.69(14)	4 815 319.78	-0.09	0.65
12	4	9	23/2	12	11	3	8	21/2	11				
18	4	14	37/2	19	17	3	15	35/2	18	5 172 050.43(77)	5 172 051.06	-0.63	0.82
18	4	14	37/2	18	17	3	15	35/2	17				
11	5	6	21/2	10	11	4	7	21/2	10	5 173 898.15(16)	5 173 898.09	0.06	0.39
11	5	7	21/2	10	11	4	8	21/2	10				
11	5	6	21/2	11	11	4	7	21/2	11				
11	5	7	21/2	11	11	4	8	21/2	11				
11	5	7	21/2	10	10	4	6	19/2	9	5 885 277.27(38)	5 885 277.60	-0.33	0.87
11	5	6	21/2	10	10	4	7	19/2	9				
11	5	7	21/2	11	10	4	6	19/2	10				
11	5	6	21/2	11	10	4	7	19/2	10				

RMS of fit = 0.25 MHz; RMS of (O-C)′ = 1.0

[a] 1σ uncertainties shown in parentheses.
[b] Transitions below 140 GHz are from Ref. (*8*), transitions from 160 to 520 GHz from Ref. (*9*), and transitions above 2400 GHz from the present work. Frequencies followed by blank columns indicate unresolved spectral structure.
[c] The ratio of O-C to the 1σ measurement error is given.
[d] Excluded from the fitting; see text for details.

wave transitions are corrected in this table. Figure 1 is a term energy diagram for HO_2, showing the transitions that are fitted in the present study.

The *A*-reduced asymmetric-top free radical Hamiltonian, including spin–rotation and nuclear hyperfine interactions, and centrifugal distortion up to high order has been developed by a number of authors (*17–20*). For analysis of the present data set, we developed a nonlinear least-squares fitting program, based upon the fitting routines in "Numerical Recipes" (*21*), to fit this form of Hamiltonian to the measured lines by full diagonalization in a parity-conserving basis set. The present work to develop a fitting procedure for this complex type of molecular Hamiltonian, borrows heavily from that of Sears (*22, 23*). 3-*j*, 6-*j*, and 9-*j* symbols were calculated using the library functions given in Zare (*24*). Explicit matrix elements for the rotation and spin–

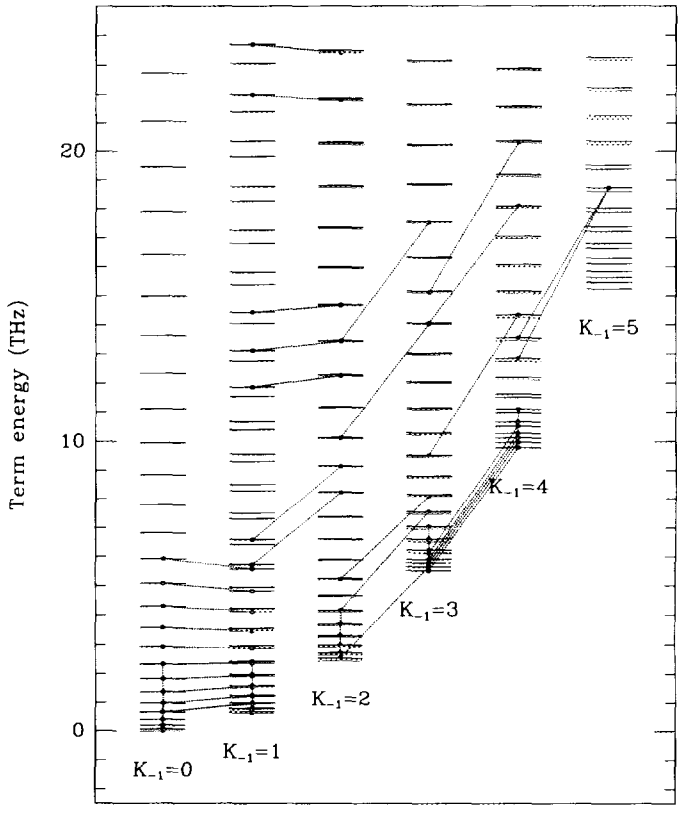

FIG. 1. Term values for the first 6 K_{-1} stacks for HO_2. The hyperfine structure and much of the asymmetry doubling are not resolved at the scale of the figure. The transitions used in the present fitting, including those from Refs. (*8, 9*) are indicated as dotted lines connecting the appropriate states.

rotation terms of the Hamiltonian expression are given in the Appendix, which is included to provide a convenient reference to the necessary matrix elements for analysis of an asymmetric top free radical.

The fitting of the measured set of transitions is complicated by the fact that nuclear hyperfine structure, asymmetry doubling, or both may not be resolved in the measured spectra (the splittings are comparable to or less than the Doppler widths of the lines). In order to perform a fit on such data, a boot-strapping procedure is necessary: A set of splittings and relative line intensities must be assumed from previous knowledge of the spectrum (*9, 10*) to provide hypothetical fully resolved transition frequencies as input to the fit. The necessary splittings are applied to the relevant transitions in the input data set, and the splitting assumptions checked at the end of the fitting process. After one iteration of this process the maximum difference between the assumed splitting difference applied to the input data and the final result is 0.2 kHz. Measured transition frequencies are weighted as the squares of the inverses of their respective uncertainties in the Hamiltonian fitting procedure. Two of the microwave transition frequencies, marked in Ref. (*8*) as being disturbed by interference, are omitted from the final fitting.

The results of the nonlinear least-squares fit of the parameterized Hamiltonian to the transition frequencies are given in Table I. We include both the differences between

the observed and calculated frequencies and their ratios to the measurement uncertainties. The rms value of the latter quantity is 1.0, indicating that the fitting model reproduces the data to the level of the measurement uncertainties. The spectroscopic constants derived from fitting the combined data set are presented in Table II. We have kept enough significant figures in these constants to reproduce the full double-precision results of the least-squares fit to 35 kHz. Inclusion of additional terms in the Hamiltonian expression, including all terms up to sextic in the rotation and the spin–rotation interaction, was investigated. (L_K was the only octic rotational constant considered.) Only constants that were statistically significant are retained in the final fit presented here. The constant Δ_{NK}^S appears in terms of the spin–rotation Hamiltonian off-diagonal by 1 in K, while the sum $\Delta_{NK}^S + \Delta_{KN}^S$ appears in diagonal terms. They were found to be highly negatively correlated, and $\Delta_{NK}^S + \Delta_{KN}^S$ is small and determined with a low degree of significance. Therefore, $\Delta_{NK}^S + \Delta_{NK}^S$ was constrained to 0 in the fit, and Δ_{NK}^S was varied.

4. DISCUSSION

The new Hamiltonian terms included in the present fitting including an octic centrifugal distortion constant L_K, a sextic spin–rotation centrifugal distortion constant Φ_K^S, and the off-diagonal component of the proton nuclear hyperfine spin–spin dipolar tensor T_1^2. The far-infrared measurements do not resolve the splittings for the $\Delta F = 1$ multiplets and do not include $\Delta F = 0$ lines. The only information on the hyperfine

TABLE II

Spectral Constants for HO_2 Ground State (MHz) from Simultaneous Fit of 173 Lines from 27 GHz to 5.9 THz

Constant	Value	σ	Constant	Value	σ
$A-(B+C)/2$	577 680.515	0.031	a_0	16 662.282	0.069
$(B+C)/2$	32 592.7356	0.0017	a_s	16 455.122	0.050
$(B-C)/4$	462.5296	0.0088	b_s	215.941	0.024
Δ_N	0.116 908	0.000 011	d_s	194.20	0.18
Δ_{NK}	3.445 72	0.000 29	Δ_K^S	23.756	0.027
Δ_K	123.5906	0.0061	Δ_{NK}^S	0.2706	0.0021
$\delta_N \times 10^3$	6.1391	0.0028	δ_K^S	0.213	0.012
δ_K	2.0062	0.0090	$\Phi_K^S \times 10^2$	-3.44	0.12
$\Phi_{NK} \times 10^5$	1.925	0.049	a_F	-27.528	0.075
$\Phi_{KN} \times 10^3$	1.086	0.015	T_0^2	-4.166	0.045
Φ_K	0.100 38	0.000 40	T_1^2	-7.2	1.4
$L_K \times 10^4$	-1.717	0.079	T_2^2	6.414	0.026

$a_0 = -1/3\,(\epsilon_{aa} + \epsilon_{bb} + \epsilon_{cc})$
$a_s = -1/6\,(2\epsilon_{aa} - \epsilon_{bb} - \epsilon_{cc})$
$b_s = -1/2\,(\epsilon_{bb} - \epsilon_{cc})$
$d_s = -1/2\,(\epsilon_{ab} + \epsilon_{ba})$

$T_0^2 = 1/2\,T_{aa} = -1/2\,(T_{bb} + T_{cc}) = 1/6\,(2T_{aa} - T_{bb} - T_{cc})$
$T_1^2 = -T_{-1}^2 = -6^{-1/2}\,T_{ba}$
$T_2^2 = 24^{-1/2}\,(T_{bb} - T_{cc})$

interactions they provide is the very limited amount implicit in the shifts of the $\Delta F = 1$ lines with respect to $\Delta F = 0$. It was possible to obtain T_1^2 in the present study because of the refitting of all available data, particularly the millimeter-wave data from Charo and De Lucia (*9*), by full diagonalization in a complete basis set. The fitted molecular constants are generally in good agreement with, and somewhat more accurate than, the best previous determinations (rotation and spin–rotation from Ref. (*9*) and hyperfine interaction parameters from Barnes *et al.* (*25*)). The spin–rotation parameters a_0, a_s, and b_s agree only at the 3σ level, while the spin–rotation centrifugal distortion parameters Δ_K^S, Δ_{NK}^S, and δ_K^S differ substantially. Δ_K^S comes into 3σ agreement when the next higher-order expansion term Φ_K^S in K is omitted from the fitting.

The hyperfine terms a_F (Fermi contact) and T_0^2 and T_2^2 (diagonal spin–spin dipolar interaction) are in excellent agreement with those from the EPR study of Ref. (*25*). The additional term T_1^2 derived in this study indicates the orientation of the principal axes of the dipole–dipole interaction tensor relative to the molecule (*26*), which can provide information on the distribution of the unpaired electron density (*27*). The present fitting process is able to confirm that d_s and T_1^2 (and, thus, the effective off-diagonal spin–rotation parameter $(\tilde{\epsilon}_{ab} + \tilde{\epsilon}_{ba})/2$ (*20*) and T_{ab}, the off-diagonal component of the Cartesian spin–spin dipolar tensor) are opposite in sign, but an arbitrary overall sign choice, which cannot be determined directly from studies of HO_2 alone, remains. Studies of the spectrum of DO_2, in comparison with HO_2 (*28*), and of the isotopic dependence of the spin–rotation interaction (*29*) have addressed the question of the sign of $(\tilde{\epsilon}_{ab} + \tilde{\epsilon}_{ba})/2$ in some detail, but with results that are not conclusive. Reference (*29*) determines values of the actual spin–rotation parameters ϵ_{ab} and ϵ_{ba}, fitted with a constraint on their independence. Use of these values indicates that the transformed parameter $(\tilde{\epsilon}_{ab} + \tilde{\epsilon}_{ba})/2$ (see Eqs. (22) and (23) of Ref. (*20*)) is probably negative, but this is inconclusive because of the constraint and the relatively high uncertainty (taken on ϵ_{ab}). Reference (*28*) determines conclusively that ϵ_{ab} is positive (in contradiction to the result in Ref. (*29*)) and that ϵ_{ba} is negative. $(\tilde{\epsilon}_{ab} + \tilde{\epsilon}_{ba})/2$ calculated with these results is negative, but a positive value of the correct magnitude is possible with values of ϵ_{ab} and ϵ_{ba} that are within the stated error bounds. We conclude that the overall sign of $(\tilde{\epsilon}_{ab} + \tilde{\epsilon}_{ba})/2$, and thus of T_{ab}, remains ambiguous, although a negative $(\tilde{\epsilon}_{ab} + \tilde{\epsilon}_{ba})/2$ and a positive T_{ab} seem more likely. Saito *et al.* (*26*) estimate a value of $|T_{ab}| = 18.3(10.8)$ MHz from comparative studies of HO_2 and DO_2, a number which is in almost fortuitous agreement with the value of 17.6(3.4) MHz determined here. They assume that T_{ba} is negative so that the principal axes of the spin–spin dipolar interaction tensor are rotated 26.3° from the inertial axes of the molecule, in the sense corresponding to a principal B axis 8.7° from the OH bond, outside the O–O–H internal angle, using the best available molecular structure (*30*). Our values for the tensor elements, $T_{aa} = -8.33(9)$ MHz, $T_{bb} = 19.88(16)$ MHz, and $|T_{ab}| = 17.6(3.4)$, correspond to a rotation of $25.6°^{+2.6}_{-2.9}$. A negative T_{ab} locates the principal B axis 8.1° from the OH bond, outside O–O–H, whereas the more likely positive value of T_{ab} locates it 43.2° from the OH bond, inside O–O–H.

In Table III we present values for the rotation frequencies of HO_2 corresponding to the transitions measured in atmospheric studies (*1–3, 6*), as well as for the lowest a- and b-type transitions, which are potentially useful for measurements of astronomical HO_2.

APPENDIX: EXPLICIT MATRIX ELEMENTS

The Hamiltonian expression is given by

$$H = H_R + H_{SR} + H_{HFS} + H_Q, \tag{2}$$

TABLE III

Selected HO_2 Lines

N′	K'_{-1}	K'_1	J′	F′	N″	K''_{-1}	K''_1	J″	F″	Frequency (MHz)
Transitions for ground-based measurements										
4	1	3	9/2	5	3	1	2	7/2	4	265 770.16
4	1	3	9/2	4	3	1	2	7/2	3	265 769.18
4	2	2	9/2	5	3	2	1	7/2	4	265 731.66
4	2	3	9/2	5	3	2	2	7/2	4	265 690.63
Lowest a- and b-type transitions										
1	0	1	3/2	1	0	0	0	1/2	0	65 070.88
1	0	1	3/2	2	0	0	0	1/2	1	65 081.81
1	0	1	3/2	1	0	0	0	1/2	1	65 098.41
1	0	1	1/2	1	0	0	0	1/2	0	65 373.05
1	0	1	1/2	0	0	0	0	1/2	1	65 396.31
1	0	1	1/2	1	0	0	0	1/2	1	65 400.58
1	1	1	3/2	1	0	0	0	1/2	0	626 580.05
1	1	1	3/2	2	0	0	0	1/2	1	626 587.19
1	1	1	3/2	1	0	0	0	1/2	1	626 607.58
1	1	1	1/2	1	0	0	0	1/2	0	666 569.32
1	1	1	1/2	0	0	0	0	1/2	1	666 574.42
1	1	1	1/2	1	0	0	0	1/2	1	666 596.85
Transitions for the Submillimeterwave Limb Sounder										
10	1	9	21/2	10	10	0	10	21/2	10	625 660.74
10	1	9	21/2	11	10	0	10	21/2	11	625 664.21
Transitions for SAO and IROE balloon-borne measurements										
4	4	1	9/2	4	3	3	0	7/2	3	4 258 492.37
4	4	0	9/2	4	3	3	1	7/2	3	4 258 492.37
4	4	1	9/2	5	3	3	0	7/2	4	4 258 492.46
4	4	0	9/2	5	3	3	1	7/2	4	4 258 492.46
4	4	1	9/2	4	3	3	0	7/2	4	4 258 510.37
4	4	0	9/2	4	3	3	1	7/2	4	4 258 510.38
4	4	1	7/2	3	3	3	0	5/2	3	4 306 794.52
4	4	0	7/2	3	3	3	1	5/2	3	4 306 794.52
4	4	1	7/2	3	3	3	0	5/2	2	4 306 809.88
4	4	0	7/2	3	3	3	1	5/2	2	4 306 809.89
4	4	1	7/2	4	3	3	0	5/2	3	4 306 810.45
4	4	0	7/2	4	3	3	1	5/2	3	4 306 810.46
5	4	2	11/2	6	4	3	1	9/2	5	4 324 315.46
5	4	1	11/2	6	4	3	2	9/2	5	4 324 315.50
5	4	2	11/2	5	4	3	1	9/2	4	4 324 315.66
5	4	1	11/2	5	4	3	2	9/2	4	4 324 315.69
5	4	2	11/2	5	4	3	1	9/2	5	4 324 331.82
5	4	1	11/2	5	4	3	2	9/2	5	4 324 331.86

where H_R is the asymmetric top rotational Hamiltonian, including centrifugal distortion, H_{SR} is the electron spin–rotation interaction, including centrifugal distortion, H_{HFS} is the nuclear hyperfine Hamiltonian, including Fermi contact and spin–spin dipolar interactions, and H_Q is the nuclear electric quadrupole interaction (e.g., for DO_2). The derivation of the matrix elements is discussed in detail in Refs. (*17–20, 22*). Hyperfine and nuclear quadrupole terms are exactly as given in Ref. (*18*), so

TABLE III—*Continued*

N′	K'_{-1}	K'_1	J′	F′	N″	K''_{-1}	K''_1	J″	F″	Frequency (MHz)
Transitions for SAO and IROE balloon-borne measurements										
5	4	2	9/2	4	4	3	1	7/2	4	4 371 249.35
5	4	1	9/2	4	4	3	2	7/2	4	4 371 249.40
5	4	2	9/2	4	4	3	1	7/2	3	4 371 262.80
5	4	1	9/2	4	4	3	2	7/2	3	4 371 262.84
5	4	2	9/2	5	4	3	1	7/2	4	4 371 263.64
5	4	1	9/2	5	4	3	2	7/2	4	4 371 263.69
6	4	3	13/2	7	5	3	2	11/2	6	4 390 319.31
6	4	2	13/2	7	5	3	3	11/2	6	4 390 319.47
6	4	3	13/2	6	5	3	2	11/2	5	4 390 319.58
6	4	2	13/2	6	5	3	3	11/2	5	4 390 319.74
6	4	3	13/2	6	5	3	2	11/2	6	4 390 334.66
6	4	2	13/2	6	5	3	3	11/2	6	4 390 334.82
8	4	5	15/2	7	7	3	4	13/2	7	4 561 975.92
8	4	4	15/2	7	7	3	5	13/2	7	4 561 977.29
8	4	5	15/2	7	7	3	4	13/2	6	4 561 987.70
8	4	5	15/2	8	7	3	4	13/2	7	4 561 988.32
8	4	4	15/2	7	7	3	5	13/2	6	4 561 989.07
8	4	4	15/2	8	7	3	5	13/2	7	4 561 989.69
9	4	6	19/2	10	8	3	5	17/2	9	4 587 971.75
9	4	6	19/2	9	8	3	5	17/2	8	4 587 972.00
9	4	5	19/2	10	8	3	6	17/2	9	4 587 974.54
9	4	5	19/2	9	8	3	6	17/2	8	4 587 974.79
9	4	6	19/2	9	8	3	5	17/2	9	4 587 985.52
9	4	5	19/2	9	8	3	6	17/2	9	4 587 988.31
10	4	7	21/2	11	9	3	6	19/2	10	4 653 554.19
10	4	7	21/2	10	9	3	6	19/2	9	4 653 554.42
10	4	6	21/2	11	9	3	7	19/2	10	4 653 559.81
10	4	6	21/2	10	9	3	7	19/2	9	4 653 560.04
10	4	7	21/2	10	9	3	6	19/2	10	4 653 567.67
10	4	6	21/2	10	9	3	7	19/2	10	4 653 573.29
11	4	8	23/2	12	10	3	7	21/2	11	4 718 959.15
11	4	8	23/2	11	10	3	7	21/2	10	4 718 959.37
11	4	7	23/2	12	10	3	8	21/2	11	4 718 969.66
11	4	7	23/2	11	10	3	8	21/2	10	4 718 969.87
11	4	8	23/2	11	10	3	7	21/2	11	4 718 972.40
11	4	7	23/2	11	10	3	8	21/2	11	4 718 982.91

they are not included here. The spins are coupled as $N + S = J$; $J + I = F$, where N is the rotational angular momentum, S is the electron spin angular momentum, I is the nuclear spin angular momentum, and F is the resultant total angular momentum. $\delta_{F'F}\delta_{J'J}$ is implied for all matrix elements given here. The explicit matrix elements in the symmetric top basis set for the A-reduced form of the Hamiltonian are

$$\langle NK|H_R|NK\rangle = \left(\frac{B+C}{2}\right)N(N+1) + \left[A - \left(\frac{B+C}{2}\right)\right]K^2 - \Delta_K K^4$$
$$- \Delta_{NK}K^2N(N+1) - \Delta_N N^2(N+1)^2 + \Phi_K K^6 + \Phi_{KN}K^4N(N+1)$$
$$+ \Phi_{NK}K^2N^2(N+1)^2 + \Phi_N N^3(N+1)^3 + L_K K^8 \quad (3)$$

$$\langle NK|H_R|NK\pm 2\rangle = \left\{\left(\frac{B-C}{4}\right) - \frac{\delta_K}{2}[K^2 + (K\pm 2)^2] - \delta_N N(N+1) + \frac{\phi_K}{2}[K^4 + (K\pm 2)^4] + \frac{\phi_{NK}}{2}N(N+1)[K^2 + (K\pm 2)^2] + \phi_N N^2(N+1)^2\right\}F(N,\pm K) \quad (4)$$

$$\langle NK|H_{SR}|NK\rangle = -\frac{a_o}{2}C(N) + \left\{a_s[3K^2 - N(N+1)] - \Delta_K^S K^4 - \Phi_K^S K^6 - (\Delta_{NK}^S + \Delta_{KN}^S)K^2 N(N+1) - \Delta_N^S N^2(N+1)^2\right\}\Theta(N) \quad (5)$$

$$\langle NK|H_{SR}|NK\pm 1\rangle = d_s(K\pm 1/2)f(N,\pm K)\Theta(N) \quad (6)$$

$$\langle NK|H_{SR}|NK\pm 2\rangle = \left\{\frac{b_s}{2} - \delta_N^S N(N+1) - \frac{\delta_K^S}{2}[K^2 + (K\pm 2)^2]\right\}\Theta(N)F(N,\pm K) \quad (7)$$

$$\langle NK|H_{SR}|N-1K\rangle = \frac{K}{2}(-3a_s + \Delta_K^S K^2 + \Delta_{NK}^S N^2 + \Phi_K^S K^4)(N^2-K^2)^{1/2}\phi(N) \quad (8)$$

$$\langle NK|H_{SR}|N-1K\pm 1\rangle = -\frac{d_s}{4}(N\pm 2K+1)g(N,\pm K)\phi(N) \quad (9)$$

$$\langle NK|H_{SR}|N-1K\pm 2\rangle = \{\mp b_s + \delta_K^S[K(N\pm K) + (K\pm 2)(N\pm K+2)\} \times f(N,\pm K)g(N,\pm K+1)\frac{\phi(N)}{4}. \quad (10)$$

Functions

$$f(x,y) = [(x-y)(x+y+1)]^{1/2} \quad (11)$$

$$g(x,y) = [(x-y)(x-y-1)]^{1/2} \quad (12)$$

$$F(N,\pm K) = \{[N(N+1) - K(K\pm 1)][N(N+1) - (K\pm 1)(K\pm 2)]\}^{1/2} = f(N,\pm K)f(N,\pm K+1) \quad (13)$$

$$C(N) = J(J+1) - N(N+1) - S(S+1) \quad (14)$$

$$\Theta(N) = -C(N)/2N(N+1) \quad (15)$$

$$P(N) = (N-J+S)(N+J+S+1) \quad (16)$$

$$Q(N) = (S+J-N)(N+J-S+1) \quad (17)$$

$$\phi(N) = -\frac{1}{N}\left\{\frac{P(N)Q(N-1)}{(2N-1)(2N+1)}\right\}^{1/2}. \quad (18)$$

Basis Set

A parity-conserving combination of symmetric top rotational wave functions is used:

$$|NK\rangle^{\pm} = \frac{1}{\sqrt{2}}(|N, K\rangle \pm (-1)^{N-K}|N, -K\rangle; \tag{19}$$

$$|N0\rangle^{+\text{or}-} = |N0\rangle(\exists \text{ for parity} = (-1)^N). \tag{20}$$

$\langle N'K|H|NK\rangle = (-1)^{N'-N}\langle N', -K|H|N, -K\rangle$, useful for calculating $\langle N'1|H|N1\rangle$, where a $\Delta K = 2$ component arises from $K = 1 \leftrightarrow K = -1$. Also, $\langle \gamma'K'|H|\gamma 0\rangle$ is multiplied by $\sqrt{2}$ for $K' = 1$ or 2, due to the nondegeneracy of the $|N0\rangle$ symmetric top wavefunction.

ACKNOWLEDGMENTS

We are grateful to T. J. Sears and J. M. Brown for valuable discussions and patient explanation on the subject of fitting the free radical asymmetric top Hamiltonian. We thank D. A. Ramsay for information on the ongoing spectroscopic study of HO_2. The research at the Smithsonian Astrophysical Observatory and the University of Oregon was supported by NASA Grant NAGW 1292. Additional support at the University of Oregon was provided by the NASA Langley Research Center Grant NAG-1-1650. The research at the National Institute of Standards and Technology was partially supported by NASA Grant W-18, 623. F. Stroh was supported for this research by a NATO fellowship administered by the Deutscher Akademischer Austauschdienst.

RECEIVED: February 1, 1995

REFERENCES

1. W. A. TRAUB, D. G. JOHNSON, AND K. V. CHANCE, *Science* **247,** 446–449 (1990).
2. J. H. PARK AND B. CARLI, *J. Geophys. Res.* **96,** 22,535–22,541 (1991).
3. R. A. STACHNIK, J. C. HARDY, J. A. TARSALA, AND J. W. WATERS, *Geophys. Res. Lett.* **19,** 1931–1934 (1992).
4. R. M. STIMPFLE, P. O. WENNBERG, L. B. LAPSON, AND J. G. ANDERSON, *Geophys. Res. Lett.* **17,** 1905–1908 (1990).
5. G. ASRAR AND D. J. DOKKEN, (Eds.), "1993 Eos Reference Handbook," NASA Publication NP-202 (1993); available from Earth Science Support Office, Document Resource Facility, 300 D Street NW, Suite 840, Washington, DC 20024.
6. R. L. DE ZAFRA, A. PARRISH, P. M. SOLOMON, AND J. W. BARRETT, *J. Geophys. Res.* **89,** 1321–1326 (1984).
7. Y. BEERS AND C. J. HOWARD, *J. Chem. Phys.* **63,** 4212–4216 (1975).
8. S. SAITO, *J. Mol. Spectrosc.* **65,** 229–238 (1977).
9. A. CHARO AND F. C. DE LUCIA, *J. Mol. Spectrosc.* **94,** 426–436 (1982).
10. R. L. POYNTER, H. M. PICKETT, AND E. A. COHEN, *Appl. Opt.* **24,** 2235–2240 (1985).
11. K. CHANCE, P. DE NATALE, M. BELLINI, M. INGUSCIO, G. DI LONARDO, AND L. FUSINA, *J. Mol. Spectrosc.* **163,** 67–70 (1994).
12. T. D. VARBERG AND K. M. EVENSON, *Astrophys. J. Lett.* **385,** 763–765 (1992).
13. K. M. EVENSON, D. A. JENNINGS, AND F. R. PETERSON, *J. Appl. Phys.* **44,** 576–578 (1984).
14. K. M. EVENSON, D. A. JENNINGS, K. R. LEOPOLD, AND L. R. ZINK, *in* "Laser Spectroscopy VII" (T. W. Haensch and Y. R. Shen Eds.), Springer Series in Optical Sciences 49, pp. 366–370, Springer-Verlag, New York, 1985.
15. K. V. CHANCE, D. A. JENNINGS, K. M. EVENSON, M. D. VANEK, I. G. NOLT, J. V. RADOSTITZ, AND K. PARK, *J. Mol. Spectrosc.* **146,** 375–380 (1991).
16. K. V. CHANCE, T. D. VARBERG, K. PARK, AND L. R. ZINK, *J. Mol. Spectrosc.* **162,** 120–126 (1993).
17. W. T. RAYNES, *J. Chem. Phys.* **41,** 3020–3032 (1964).
18. I. C. BOWATER, J. M. BROWN, AND A. CARRINGTON, *Proc. R. Soc. London A* **333,** 265–288 (1973).
19. J. M. BROWN AND T. J. SEARS, *Mol. Phys.* **34,** 1595–1610 (1977).
20. J. M. BROWN AND T. J. SEARS, *J. Mol. Spectrosc.* **75,** 111–133 (1979).
21. W. H. PRESS, B. P. FLANNERY, S. A. TEUKOLSKY, AND W. T. VETTERLING, "Numerical Recipes," Cambridge Univ. Press, Cambridge, UK, 1986.
22. T. J. SEARS, *Comput. Phys. Rep.* **3,** 1–32 (1984).

23. T. J. SEARS, *Comput. Phys. Commun.* **34,** 123–133 (1984).
24. R. N. ZARE, "Angular Momentum," Wiley-Interscience, New York, 1988.
25. C. E. BARNES, J. M. BROWN, A. CARRINGTON, J. PINKSTONE, T. J. SEARS, AND P. J. THISTLETHWAITE, *J. Mol. Spectrosc.* **72,** 86–101 (1978).
26. S. SAITO, Y. ENDO, AND E. HIROTA, *J. Mol. Spectrosc.* **98,** 138–145 (1983).
27. F. J. ADRIAN, E. L. COCHRAN, AND V. A. BOWERS, *J. Chem. Phys.* **47,** 5441–5442 (1967).
28. T. J. SEARS, G. A. TAKACS, C. J. HOWARD, R. L. CROWNOVER, P. HELMINGER, AND F. C. DE LUCIA, *J. Mol. Spectrosc.* **118,** 103–120 (1986).
29. J. M. BROWN, T. J. SEARS, AND J. K. G. WATSON, *Mol. Phys.* **41,** 173–182 (1980).
30. C. E. BARNES, J. M. BROWN, AND H. E. RADFORD, *J. Mol. Spectrosc.* **84,** 179–196 (1980).